Article

Tackling Pseudomonas aeruginosa Virulence by a Hydroxamic Acid-Based LasB Inhibitor

Andreas M. Kany, asfandyar sikandar, Samir Yahiaoui, Jörg Haupenthal, Isabell Walter, Martin Empting, Jesko Koehnke, and Rolf W. Hartmann

ACS Chem. Biol., **Just Accepted Manuscript** • DOI: 10.1021/acschembio.8b00257 • Publication Date (Web): 08 Aug 2018

Tackling *Pseudomonas aeruginosa* Virulence by a Hydroxamic Acid-Based LasB Inhibitor

Andreas M. Kany[†], Asfandyar Sikandar[‡], Samir Yahiaoui[†], Jörg Haupenthal[†], Isabell Walter[†], Martin Empting[†], Jesko Köhnke[‡], Rolf W. Hartmann[*,†,§]

[†] Helmholtz Institute for Pharmaceutical Research Saarland (HIPS), Department of Drug Design and Optimization, Campus E8.1, 66123, Saarbrücken, Germany

[‡] Helmholtz Institute for Pharmaceutical Research Saarland (HIPS), Workgroup Structural Biology of Biosynthetic Enzymes, Campus E8.1, 66123, Saarbrücken, Germany

[§] Department of Pharmacy, Pharmaceutical and Medicinal Chemistry, Saarland University, Campus E8.1, 66123 Saarbrücken, Germany

* Rolf.Hartmann@helmholtz-hzi.de

ABSTRACT

In search of novel antibiotics to combat the challenging spread of resistant pathogens, bacterial proteases represent promising targets for pathoblocker development. A common motif for protease inhibitors is the hydroxamic acid function, yet this group has often been related to unspecific inhibition of various metalloproteases. In this work, the inhibition of LasB, a harmful zinc metalloprotease secreted by *Pseudomonas aeruginosa*, through a hydroxamate derivative is described. The present inhibitor was developed based on a recently reported, highly selective thiol scaffold. Using X-ray crystallography, the lack of inhibition of a range of human matrix-metalloproteases could be attributed to a distinct binding mode sparing the S1´ pocket. The inhibitor was shown to restore the effect of the antimicrobial peptide LL-37, to reduce the formation of *P. aeruginosa* biofilm and, for the first time for a LasB inhibitor, the release of extracellular DNA. Hence, it is capable of disrupting several important bacterial resistance mechanisms. These results highlight the potential of protease inhibitors to fight bacterial infections and point out the possibility to achieve selective inhibition even with a strong zinc anchor.

Proteases have proven to be attractive targets for the treatment of various diseases, including infections.[1] While antiviral protease inhibitors are in clinical use for the treatment of e.g. HIV or HCV, no bacterial protease inhibitors have been approved as anti-infective drugs yet.[2,3] However, in order to combat the spread of antibiotic resistance, new antibacterial agents with novel modes of action are

urgently needed.[4–6] This applies especially for Gram-negative pathogens which are challenging to treat as their cell wall is difficult to permeate.[7] The development of pathoblockers which target bacterial virulence rather than killing bacteria is of growing interest in anti-infective drug discovery, due to the reduced selection pressure such a strategy is supposed to have.[8–12] In this context, bacterial proteases represent attractive targets.[2,3,13] Notably, the only FDA-approved anti-virulence drugs are immunoglobulins that target secreted virulence factors, highlighting the potential of extracellular targets to circumvent cell wall permeation problems.[8] The highly problematic Gram-negative pathogen *Pseudomonas aeruginosa* has been assigned critical priority by the WHO[14] and urgently requires novel treatment options because of increasing resistance.[15,16] *P. aeruginosa* is i.a. responsible for fatal lung infections in cystic fibrosis patients.[17] Among its numerous virulence factors representing potential drug targets,[12,16,18–20] the zinc-metalloprotease elastase (LasB) is of specific interest, given its extracellular location.[21] LasB substantially contributes to disease progression in *P. aeruginosa* infected individuals by facilitating host invasion and immune evasion.[22] It was for example found to degrade and thereby inactivate the endogenous antimicrobial peptide (AMP) LL-37.[23] Furthermore, LasB was reported to be involved in the formation of *P. aeruginosa* biofilms either by periplasmic activation of nucleoside diphosphate kinase (NDK) required for alginate synthesis[24], or by upregulation of rhamnolipids.[25] The aggregation of bacteria in the biofilm matrix seriously impedes successful antibiotic treatment and blocks host defense mechanisms.[26,27]

Several thiol-based inhibitors with promising activity on LasB have been described.[28–32] A class of *N*-aryl mercaptoacetamides turned out to be particularly attractive since these thiols display high selectivity against a range of human matrix metalloproteinases (MMPs).[32,33] Thiol-containing compounds are in clinical use for the treatment of various diseases.[34–36] However, a disadvantage of this class compared to other zinc-chelating inhibitors is the possible oxidation to the respective disulfides, resulting in inactivation of the compounds.[37]

In this study, we describe the synthetic replacement of the sulfhydryl function of LasB inhibitor **1**[32] (IC_{50}: 6.6 ± 0.3 µM) by zinc-binding groups insensitive to oxidation (Figure 1). Among the compounds tested, a hydroxamic acid derivative was found to inhibit LasB in the low micromolar range as well. Hydroxamates have been reported as LasB inhibitors, but the described compounds lack selectivity against human MMPs.[38,39] In contrast, the inhibitor described in this work maintained the remarkable selectivity of thiol **1** against human MMPs, despite a binding mode equivalent to described hydroxamate-MMP complexes. The new compound was further able to reduce biofilm formation and eDNA release by *P. aeruginosa* and to restore the antimicrobial effect of LL-37.

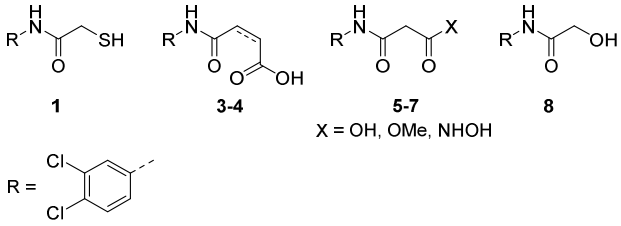

Figure 1. Structures of lead LasB inhibitor **1** and compounds **3–8** synthesized in this article.

RESULTS AND DISCUSSION

Synthesis of novel compounds 3–8.

Among the variety of chemically diverse zinc binding groups in literature,[40] we focused on hydroxyl, carboxyl and hydroxamate functions. By introducing these relatively small zinc chelating groups, drastic changes in the size of the thiol function of **1** were avoided in order to allow the inhibitor backbone to preserve the previously observed binding mode.[32] Carboxylic acid derivatives **3**, **4** and **6** were obtained either by reacting aniline **2** with succinic/maleic anhydride or via hydrolysis of methylester intermediate **5**. Similarly, **7** was synthesized by reacting **5** with hydroxylamine (Scheme 1, A-B). As an isosteric modification we further synthesized the alcohol derivative of **1**, compound **8**, using glycolic acid in a neat reaction (Scheme 1, C).

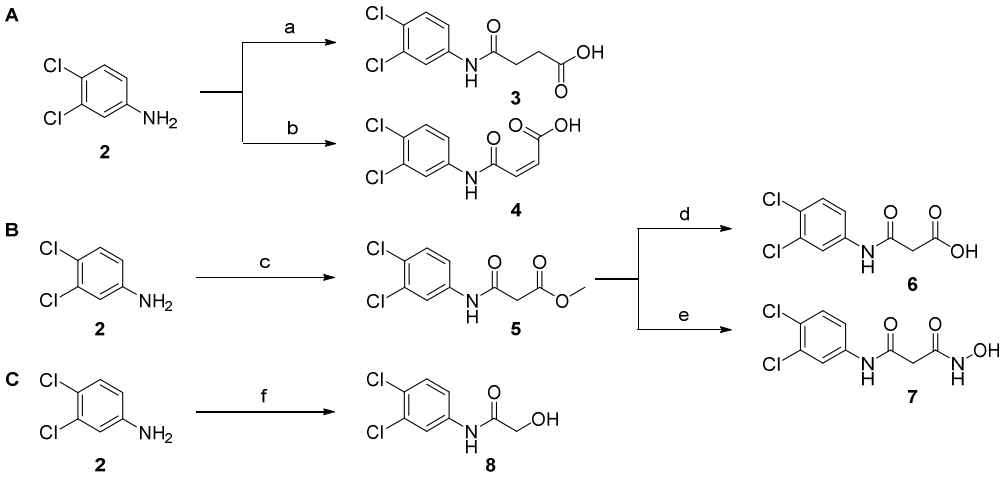

Scheme 1. Reagents and conditions: (a) succinic anhydride, dioxane, 70 °C, 6 h, (b) maleic anhydride, dioxane, 70 °C, 6 h; (c) methyl malonyl chloride, Et_3N, DCM, RT, 4 h; (d) NaOH, THF, RT, 24 h; (e) H_2NOH, DIPEA, MeOH, 8 h reflux, 16 h RT; (f) glycolic acid, 130°C, 24 h

Identification of compound 7 as a promising LasB inhibitor

Using a FRET-based inhibition assay[41] it turned out that replacement of the thiol function of **1** by a hydroxy group led to a complete loss of activity when tested at 600 µM (**8**). Compounds bearing a

carboxylic acid in γ- (**3**,**4**) or in β-position (**6**) to the carbonyl group were also inactive. Contrary to that, the activity was maintained for the β-hydroxamic acid derivative **7,** displaying an IC_{50} of 17.4 ± 0.8 µM and a $K_{i,app}$ of 12.3 ± 0.6 µM. This is slightly less active compared to the free thiol analogue **1**, however, the oxidation issue was resolved by replacing the thiol by a hydroxamic acid function.

Binding Mode of 7 to LasB.

In order to rationalize whether the minor difference in activity compared to **1** was due to a different binding mode, the X-ray co-crystal structure of the LasB-**7** complex was solved. The complex crystallized in space group $P2_12_12_1$ and crystals diffracted to 2.1 Å resolution (Figure 2, A). The structure was solved by molecular replacement using the published LasB structure (PDB ID 1EZM) as a search model. Full details of the data collection and refinement statistics can be found in Supplementary Table 1. Hydroxamate **7** was found to be orientated toward the primed binding site of the protease. As expected, the active site zinc atom is coordinated by both the carbonyl oxygen and the hydroxamide oxygen of **7**, leading to a distorted trigonal-bipyramidal geometry. The carbonyl oxygen further undergoes a weaker interaction with His223 (3.5 Å). Additionally, the hydroxamide oxygen forms a hydrogen bond with the adjacent Glu141 (2.5 Å), while the amide nitrogen interacts with the carbonyl group of Ala113 (3.0 Å). These observations are in excellent accordance with the reported binding of hydroxamate functions to MMP-7,[42] MMP-3[43] or to thermolysin.[44] Inhibitor binding to thermolysin-like proteases like LasB was described to lead to a closure of the binding pocket due to hinge-bending motion.[45] Intriguingly, thiol **1** has recently been discovered by us to keep the active site cleft in an open conformation due to the unexpected binding of two molecules to the primed binding site (Supplementary Figure S1).[32] In contrast, only one molecule of the hydroxamate binds to the protease, which undergoes the characteristic hinge-bending. Unlike the zinc-chelating thiol, the hydroxamate directly interacts with the edge strand via a hydrogen bond with the main chain oxygen of Ala113. This interaction presumably promotes closure of the active site cleft, which is hampered in case of thiol **1** by the second molecule interacting with Asn112. Due to the twisted orientation of the aromatic core of **7** compared to **1**, a previously observed bidentate hydrogen bond with Arg198 in the S1′ binding site is not possible. This observation could explain the slightly weaker activity of the hydroxamate compared to the thiol.

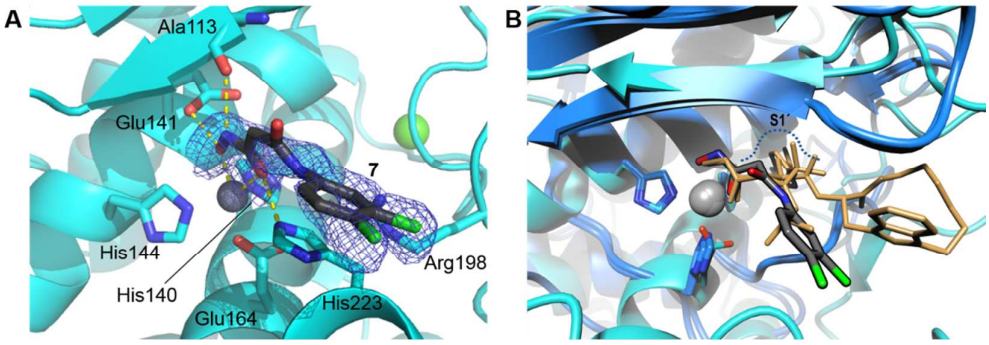

Figure 2. (A) Structure of LasB in complex with **7**. Cartoon representations of LasB (cyan) in complex with **7** (black). The difference electron density (F_o-F_c) contoured to 3σ with phases calculated from a model that was refined in the absence of **7** is shown as a blue isomesh. The active-site zinc ion is shown as a grey, calcium ion as a green sphere. Residues involved in binding of **7** are shown as sticks, their interactions depicted as yellow dashed lines. Zinc-liganding distances are 2.1 Å (OH) and 2.4 Å (NH). (B) Overlay of LasB (cyan) in complex with **7** (grey) and MMP-3/-7 (green) occupied by hydroxamate inhibitors **9** and **10** (brown, PDB codes 4G9L/1MMQ). Zinc ligands are highlighted.

Selectivity against six MMPs and ADAM-17.

Strong zinc chelating groups like hydroxamic acids can be the reason for poor selectivity against further metalloproteases, when compound binding is driven more by the chelating moiety than by the rest of the molecule.[46] In fact, the lack of selectivity against MMP anti-targets has been one reason for the failure of various hydroxamate-based MMP inhibitors in clinical trials.[47,48] Considering the high similarity in zinc chelation by **7** and the hydroxamates in MMP-3 or MMP-7, it was investigated whether the previously demonstrated selectivity of *N*-aryl mercaptoacetamides toward six human MMPs[32,33] could be maintained. Fortunately, **7** did not inhibit these MMPs comprising members with differing depth of the S1′ binding site[49] including MMP-3 and -7 (Table 1). By contrast, the unselective inhibitor Batimastat[50] (Supplementary Figure S2) inhibited all tested enzymes in the low nanomolar range.

Table 1. Residual activity of six MMPs and ADAM-17 in presence of 100 µM **7** and IC_{50} values of Batimastat[33]; Means and SD of at least two independent measurements are displayed. *: test at 25 µM. n.d.: not determined.

	7	**Batimastat**
	Residual activity at 100 µM [%]	**IC_{50} [nM]**
MMP-1	91 ± 9	2.2 ± 0.1
MMP-2	87 ± 3	1.8 ± 0.1
MMP-3	84 ± 5	5.6 ± 0.9
MMP-7	98 ± 3	7.0 ± 0.2
MMP-8	73 ± 6	0.7 ± 0.2
MMP-14	98 ± 4	2.8 ± 0.2
ADAM-17	38 ± 12	n.d.
ADAM-17	61 ± 23*	n.d.

This of course prompted the question why, despite comparable interactions of the hydroxamate function, LasB was inhibited but not MMP–7. Logically, the selectivity might be related to differences in the positioning of the inhibitor backbone in the pocket. In order to investigate this, published X-ray structures of MMPs in complex with hydroxamates were overlaid with the LasB-**7** complex. The shallow S1´ pocket of MMP-7 is occupied by an isobutyl moiety of inhibitor **9**[42] and the deep S1´ pocket of MMP-3 by an aromatic core of inhibitor **10**[43] (for inhibitor structures see Supplementary Figure S3). In contrast, the core of **7** does not bind to the respective pocket of LasB (Figure 2, B). The ability to bind the S1´ pocket of the respective MMP is a common feature of reported hydroxamate-based MMP inhibitors, which can also be the cause for a lack of selectivity.[46,51] Consequently, the high selectivity against various MMPs with differing depth of the S1´ binding pocket might be explained by an inability of **7** to bind to this site of the protease. ADAMs (A Disintegrin and Metalloproteinase), a class of zinc-dependent proteases playing essential roles in muscle development, cell migration or shedding, display additional antitargets for the presented LasB inhibitor. In this context, an *in vitro* inhibition assay toward ADAM-17 revealed that **7** exerted moderate inhibitory effects (Table 1). Consequently, further optimization regarding selectivity toward this antitarget is needed. Still, the promising selectivity toward a range of MMPs makes **7** an attractive starting point for LasB inhibitor development.

Cytotoxicity Assays.

In addition to selectivity, it was also investigated whether the cytotoxicity of **7** toward human cell lines was as low as described for thiol **1**.[32] This was of specific interest since cytotoxic properties are a known drawback of hydroxamates.[52] Notably, **7** had only low effects on the viability of HEP G2 cells, comparable to thiol **1** and rifampicin (Figure 3). The effect on HEK293 cells was more pronounced at the tested concentrations, which might be related to the inhibition of antitargets such as ADAM-17. For comparison, residual enzyme activities in the LasB *in vitro* assay are listed for each inhibitor concentration in Supplementary Table S2.

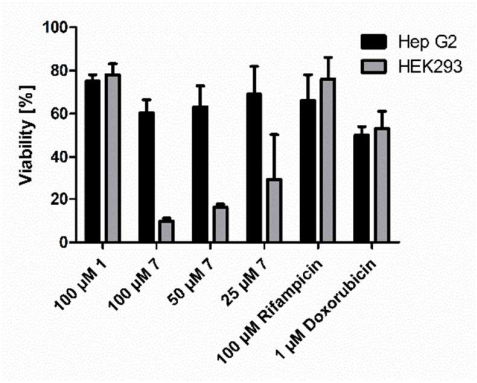

Figure 3. Cytotoxicity of **1**, **7** and two reference compounds toward HEP G2 and HEK293 cells (Values for **1** are taken from[32])

Selectivity against HDACs.

Considering the cytotoxic effects of **7** against HEP G2 cells, it was investigated whether this observation could furthermore be related to inhibition of histone deacetylases (HDACs).[53] These zinc-dependent enzymes are involved in the epigenetic regulation of cell proliferation and differentiation.[54] Given that HDACs are known to be inhibited by hydroxamic acids like vorinostat or trichostatin A,[55] assessing a potential inhibitory effect of hydroxamate **7** was of special interest. Figure 4 shows that **7** does not exert any inhibitory effect on HDAC3 and HDAC8, while these enzymes are efficiently inhibited by the positive control trichostatin A (Supplementary Figure S2). The observed selectivity against these additional antitargets could be explained by the absence of a long linker separating the zinc chelating function from the aromatic core, as it is typical for hydroxamate-based HDAC inhibitors.[52,56]

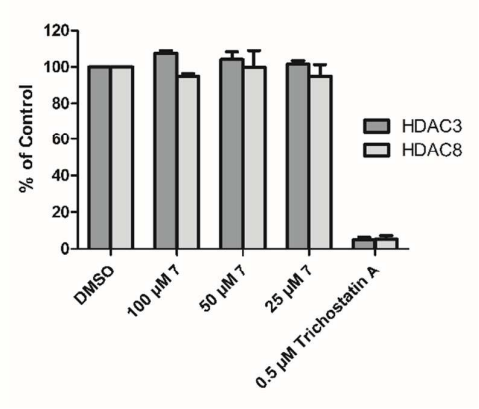

Figure 4. Residual activity of selected HDAC enzymes in presence of 100 µM 7.

Restoration of LL-37 antibacterial activity against *P. aeruginosa* PA14.

LL-37 is an α-helical human cathelicidin peptide, which shows increased prevalence in cystic fibrosis patients.[57] Its effectiveness against *P. aeruginosa* is considerably reduced as it is susceptible toward cleavage by LasB.[23] In order to assess a potential restoration effect of **7** on the activity of LL-37, a bacterial growth assay with PA14 and LL-37 in presence/absence of **7** was performed (Figure 5). The antibacterial effect of LL-37 alone was only minor at 25 µg/mL ($p = 0.0211$). However, when combined with the LasB inhibitor, it recovered its ability to reduce bacterial growth in a dose-dependent way. Significant reduction of the OD_{600} was observed starting from a hydroxamate concentration of 62.5 µM ($p = 0.0047$). At high concentrations, **7** itself slightly inhibited PA14 growth, yet to a much lower extent than in combination with LL-37 ($p = 0.0255$ at 250 µM **7**). These findings highlight the potential of LasB inhibitor **7** to restore a host defense mechanism which is otherwise hampered by LasB.

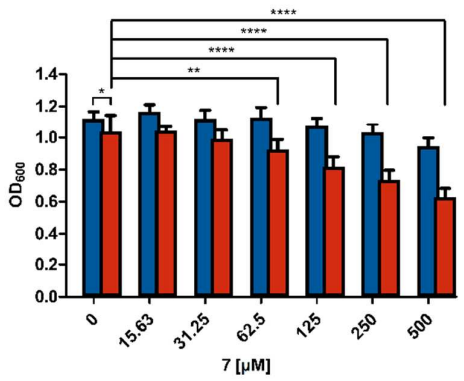

Figure 5. Growth of PA14 cultures incubated with **7** in absence (blue) and presence (red) of 25 µg/mL LL-37. Means and SD of three independent measurements are depicted. * = $p < 0.05$, ** = $p < 0.01$, **** = $p < 0.0001$

Biofilm volume and eDNA reduction

The biofilm matrix, a key element of *P. aeruginosa* resistance,[26] is composed of extracellular polysaccharides, lipids, proteins and, importantly, extracellular DNA (eDNA).[58,59] Inhibition of LasB was shown to inhibit biofilm formation.[28] Therefore, it was of great interest to investigate whether treatment of PA14 cultures with **7** would result in reduced biofilm formation as well. Indeed, the hydroxamate caused a concentration-dependent reduction of eDNA release (Figure 6, A) and of the overall biofilm volume (Figure 6, B). Since significant inhibition was observed at concentrations lower than 250 µM, these effects can be attributed to the on-target activity of the compound and are not due to a reduction of bacterial growth or lysis of cells. Hence, LasB inhibitor **7** has demonstrated important pathoblocker activity. It is able to interfere with crucial factors leading to bacterial resistance of *P. aeruginosa* toward antibiotics and host defense molecules.[27,60] To the best of our knowledge, no direct correlation between LasB inhibition and a reduction of eDNA release has been reported to date. Regarding the two mechanisms discussed in literature, the reduced biofilm formation is either due to a reduced NDK-mediated alginate synthesis,[24] or rhamolipid-mediated.[25] Which of these mechanisms inhibitor **7** interferes with cannot be concluded. Yet, these findings could hint at the capacity of 7 to permeate at least the outer membrane of the Gram-negative cell wall, as far as an inhibition of periplasmic NDK[24] is concerned.

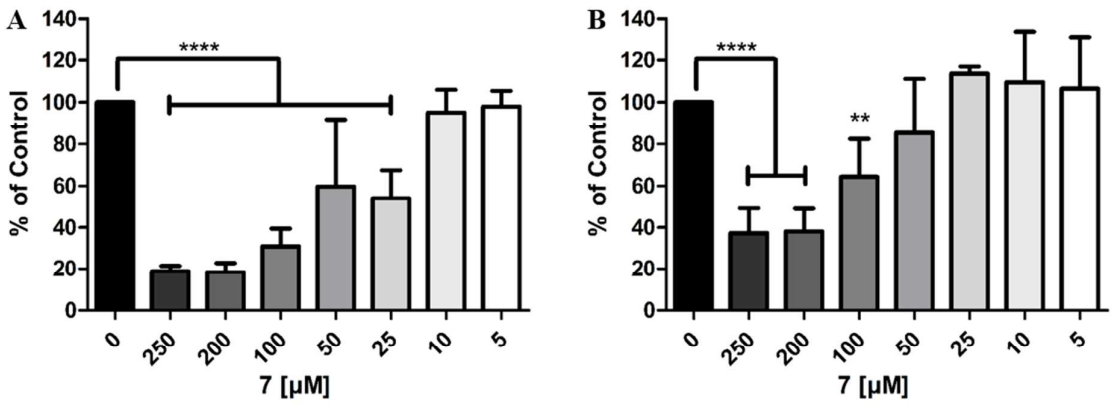

Figure 6. Reduction of eDNA release by treatment of PA14 cultures with **7**. (A) Reduction of overall PA14 biofilm volume by **7**. (B) Columns represent mean and SD of at least four independent measurements. ** = $p < 0.01$, **** = $p < 0.0001$

CONCLUSION

Based on our recent findings that *N*-aryl mercaptoacetamides are promising highly selective inhibitors of the virulence factor LasB from *P. aeruginosa*, the lead inhibitor was modified by changing the zinc-chelating moiety to a hydroxamate. Using X-ray crystallography, it was shown that similar to the thiol analogue **1**, hydroxamate **7** occupied the primed binding site. Contrary to our recent observations for **1**, only one inhibitor molecule was bound to the protease, which could undergo the characteristic hinge-bending motion resulting in a closed conformation of the enzyme. This was attributed to the ability of the inhibitor to interact with catalytic zinc and the edge strand alike. Despite the high similarity of zinc binding to hydroxamates inhibiting MMP-7, inhibitor **7** was unexpectedly able to maintain the remarkable selectivity of **1** toward a range of MMPs. This could be rationalized by the fact that the S1´ pocket was not occupied by **7**, unlike observed for MMP inhibitors. These findings show that despite the selectivity issues related to hydroxamic acids, selectivity can indeed be achieved by sparing the S1´ pocket. Since cytotoxic effects toward mammalian cell lines were observed, the activity of **7** was investigated regarding other antitargets revealing a moderate inhibition of ADAM-17 and high selectivity against HDAC3 and 8. Consequently, there will be a special focus on selectivity and cytotoxicity during future compound optimization. Below an antibacterial concentration of 250 µM, LasB was efficiently inhibited *in vitro*. This inhibition could be translated into more complex, cellular assays, highlighting this compound as a promising anti-virulence agent. After reduction of their pathogenicity by such an agent, bacteria are supposed be cleared by host defense mechanisms or with the help of conventional antibiotics.[10,11] In this context, our results highlight a direct restoration effect of the antibacterial activity of the host defense peptide AMP LL-37 *in vitro*. Indirectly, the activity of host defense mechanisms might be further improved by the inhibition of biofilm formation and eDNA release also observed for **7**. The same holds true for the effectiveness of conventional antibiotics, which is seriously hampered by bacterial biofilms. Overall, these findings show

hydroxamate **7** to be an interesting lead, which could pave the way for the rational development of selective protease inhibitors as potential new antibiotics.

METHODS.

Chemistry. All reagents were used from commercial suppliers without further purification. Procedures were not optimized regarding yield. NMR spectra were recorded on a Bruker Fourier 300 (300 MHz) spectrometer. Chemical shifts are given in parts per million (ppm) and referenced against the residual proton, ^{1}H, or carbon, ^{13}C, resonances of the >99% deuterated solvents as internal reference. Coupling constants (*J*) are given in Hertz. Data are reported as follows: chemical shift, multiplicity (s = singlet, d = doublet, t = triplet, m = multiplet, br = broad and combinations of these) coupling constants and integration. Mass spectrometry was performed on a SpectraSystems-MSQ LCMS system (Thermo Fisher). Flash chromatography was performed on silica gel 60 M, 0.04–0.063 mm (Machery-Nagel) or using the automated flash chromatography system CombiFlash Rf+ (Teledyne Isco) equipped with RediSepRf silica columns (Axel Semrau) or Chromabond Flash C18 columns (Macherey-Nagel). Purity of compounds synthesized by us was determined by LCMS using the area percentage method on the UV trace recorded at a wavelength of 254 nm and found to be >95%.

Expression and Purification of LasB. LasB was expressed and purified as described previously.[32]

***In vitro* Inhibition Assays.** The LasB *in vitro* inhibition assay and the MMP assay were performed as described previously.[32] The LasB concentration that was used in the assay was 0.3 nM. The K_m value for LasB was determined to be 363.0 µM.

ADAM Inhibition Assay. ADAM-17 (TACE) Inhibitor Screening Assay Kit was purchased from Sigma-Aldrich. The assay was performed according to the guidelines of the manufacturer. Fluorescence signals were measured in a CLARIOstar plate reader (BMG Labtech).

HDAC Inhibition Assay. HDAC3 and HDAC8 inhibitor screening kits were purchased from Sigma-Aldrich. The assay was performed according to the guidelines of the manufacturer. Fluorescence signals were measured in a CLARIOstar plate reader (BMG Labtech).

Cytotoxicity assays. Hep G2 or HEK293 cells (2 x 10^5 cells per well) were seeded in 24-well, flat-bottomed plates. Culturing of cells, incubations and OD measurements were performed as described previously[61] with small modifications. 24 h after seeding the cells the incubation was started by the addition of compounds in a final DMSO concentration of 1 %. The living cell mass was determined after 48 h. At least three independent measurements were performed for each compound.

X-ray Crystallography and image preparation. LasB was concentrated to 10–12 mg mL^{-1} and mixed with inhibitor **7** at a final concentration of 1 mM. Complex crystals were grown by the sitting

drop method using a reservoir solution containing 1.8 M $AMSO_4$ and 0.1 M Tris-Cl, pH 8.8. Crystals were cryoprotected in glycerol and diffraction data was collected from single crystals at 100 K at beamline ID29 (ESRF) at a wavelength of 1.738 Å. Data was processed using Xia2[62] and the structure solved using PHASER8[63] molecular replacement with *Pseudomonas aeruginosa* LasB (PAE, PDB ID 1EZM) as a search model. The solution was manually rebuilt with COOT[64] and refined using PHENIX[65] and Refmac5[66]. The final refined structure of LasB in complex with compound **7** was deposited in the Protein Data Bank (PDB) as entry 6FZX. Structural superimposition of complex structures of human MMPs (1MMQ and 4G9L) and LasB (6FZX) was achieved through alignment of residues 201–205 of 4G9L (corresponds to residues 140–144 of 1MMQ) using the align atoms algorithm of YASARA structure (YASARA Biosciences GmbH).[67] Image was rendered using PovRay (http://www.povray.org/).

Bacterial growth assay. The assay was performed in 96 well plates (Greiner) with a final volume of 200 µL. LL-37 was purchased from AnaSpec (Fremont) and diluted to a final concentration of 25 µg mL^{-1} from 125 µg mL^{-1} stocks in 18MΩ H_2O. Prior to culture addition **7** was serially diluted in DMSO. A pre-culture of PA14 was adjusted to the final start OD_{600} 0.02 in lysogeny broth medium. All samples contained 1% DMSO and 40% of 18MΩ H_2O. OD_{600} was measured using a FLUOstar Omega (BMG Labtech) after inoculation and after incubation for 16.5 h at 37°C with 200 rpm. Given OD_{600} values were obtained after subtraction of the respective start OD_{600} and represent three independent measurements with at least two replicates each. One-way ANOVA was performed using GraphPad Prism 6 software.

Biofilm and eDNA assays. The assays were performed as described previously.[68]

ASSOCIATED CONTENT

Supporting Information Available: This information is available free of charge *via* the Internet. Supplementary Table 1, giving X-ray data collection and refinement statistics, Supplementary Table T2, showing residual activities of LasB in the *in vitro* assay, Supplementary Figure S 1–3, showing a comparison of the LasB-**1** complex to LasB-**7** and structures of hydroxamate-based MMP inhibitors **9**, **10**, Batimastat and HDAC inhibitor Trichostatin A, synthetic procedures and spectral data for compounds **3–8**

The image of LL-37 used in the TOC graphic was created using PDB entry 2K6O.

ACKNOWLEDGEMENTS

J. Köhnke acknowledges the DFG for an Emmy-Noether Fellowship (KO 4116/3–1). We thank J. Jung, S. Amann and D. Jener for technical support and T. Röhrig for help with statistical analysis.

References

1 Turk, B. (2006) Targeting proteases. Successes, failures and future prospects. *Nat. Rev. Drug Discovery. 5*, 785–799.

2 Agbowuro, A. A., Huston, W. M., Gamble, A. B., Tyndall, J. D. A. (2017) Proteases and protease inhibitors in infectious diseases. *Med. Res. Rev.* Epub Nov 17, 2017. DOI: 10.1002/med.21475.

3 Culp, E., Wright, G. D. (2017) Bacterial proteases, untapped antimicrobial drug targets. *J. Antibiot. 70*, 366–377.

4 Cooper, M. A., Shlaes, D. (2011) Fix the antibiotics pipeline. *Nature. 472*, 32.

5 Taubes, G. (2008) The bacteria fight back. *Science. 321*, 356–361.

6 Coates, A. R. M., Halls, G., Hu, Y. (2011) Novel classes of antibiotics or more of the same? *Br. J. Pharmacol. 163*, 184–194.

7 Payne, D. J., Gwynn, M. N., Holmes, D. J., Pompliano, D. L. (2007) Drugs for bad bugs. Confronting the challenges of antibacterial discovery. *Nat. Rev. Drug Discovery. 6*, 29–40.

8 Dickey, S. W., Cheung, G. Y. C., Otto, M. (2017) Different drugs for bad bugs. Antivirulence strategies in the age of antibiotic resistance. *Nat. Rev. Drug Discovery. 16*, 457–471.

9 Heras, B., Scanlon, M. J., Martin, J. L. (2015) Targeting virulence not viability in the search for future antibacterials. *Br. J. Clin. Pharmacol. 79*, 208–215.

10 Rasko, D. A., Sperandio, V. (2010) Anti-virulence strategies to combat bacteria-mediated disease. *Nat. Rev. Drug Discovery. 9*, 117–128.

11 Clatworthy, A. E., Pierson, E., Hung, D. T. (2007) Targeting virulence. A new paradigm for antimicrobial therapy. *Nat. Chem. Biol. 3*, 541–548.

12 Kamal, A. A. M., Maurer, C. K., Allegretta, G., Haupenthal, J., Empting, M., Hartmann, R. W. (2017) Quorum Sensing Inhibitors as Pathoblockers for Pseudomonas aeruginosa Infections: A New Concept in Anti-Infective Drug Discovery. In *Topics in Medicinal Chemistry, pp* 1-26, Springer, Berlin, Heidelberg.

13 Travis, J., Potempa, J. (2000) Bacterial proteinases as targets for the development of second-generation antibiotics. *Biochim. Biophys. Acta. 1477*, 35–50.

14 World Health Organization (2017) Antibacterial Agents in Clinical Development. *An analysis of the antibacterial clinical development pipeline, including tuberculosis.* World Health Organization, Geneva.

15 Aloush, V., Navon-Venezia, S., Seigman-Igra, Y., Cabili, S., Carmeli, Y. (2006) Multidrug-resistant Pseudomonas aeruginosa. Risk factors and clinical impact. *Antimicrob. Agents Chemother. 50*, 43–48.

16 Wagner, S., Sommer, R., Hinsberger, S., Lu, C., Hartmann, R. W., Empting, M., Titz, A. (2016) Novel Strategies for the Treatment of Pseudomonas aeruginosa Infections. *J. Med. Chem. 59*, 5929–5969.

17 Sordé, R., Pahissa, A., Rello, J. (2011) Management of refractory Pseudomonas aeruginosa infection in cystic fibrosis. *Infect Drug. Resist. 4*, 31–41.

18 Storz, M. P., Maurer, C. K., Zimmer, C., Wagner, N., Brengel, C., Jong, J. C. de, Lucas, S., Müsken, M., Häussler, S., Steinbach, A., Hartmann, R. W. (2012) Validation of PqsD as an anti-biofilm target in Pseudomonas aeruginosa by development of small-molecule inhibitors. *J. Am. Chem. Soc. 134*, 16143–16146.

19 Strateva, T., Mitov, I. (2011) Contribution of an arsenal of virulence factors to pathogenesis of Pseudomonas aeruginosa infections. *Ann. Microbiol. 61*, 717–732.

20 Lu, C., Maurer, C. K., Kirsch, B., Steinbach, A., Hartmann, R. W. (2014) Overcoming the unexpected functional inversion of a PqsR antagonist in Pseudomonas aeruginosa. An in vivo potent antivirulence agent targeting pqs quorum sensing. *Angew. Chem. Int. Ed. Engl. 53*, 1109–1112.

21 Morihara, K., Tsuzuki, H., Oka, T., Inoue, H., Ebata, M. (1965) Pseudomonas aeruginosa elastase: isolation, crystallization, and preliminary characterization. *J. Biol. Chem. 240*, 3295–3304.

22 Wretlind, B., Pavlovskis, O. R. (1983) Pseudomonas aeruginosa elastase and its role in Pseudomonas infections. *Rev. Infect. Dis. 5 Suppl 5*, S998-1004.

23 Schmidtchen, A., Frick, I.-M., Andersson, E., Tapper, H., Björck, L. (2002) Proteinases of common pathogenic bacteria degrade and inactivate the antibacterial peptide LL-37. *Mol. Microbiol. 46*, 157–168.

24 Kamath, S., Kapatral, V., Chakrabarty, A. M. (1998) Cellular function of elastase in Pseudomonas aeruginosa. Role in the cleavage of nucleoside diphosphate kinase and in alginate synthesis. *Mol. Microbiol. 30*, 933–941.

25 Yu, H., He, X., Xie, W., Xiong, J., Sheng, H., Guo, S., Huang, C., Di Zhang, Zhang, K. (2014) Elastase LasB of Pseudomonas aeruginosa promotes biofilm formation partly through rhamnolipid-mediated regulation. *Can. J. Microbiol. 60*, 227–235.

26 Høiby, N., Bjarnsholt, T., Givskov, M., Molin, S., Ciofu, O. (2010) Antibiotic resistance of bacterial biofilms. *Int. J. Antimicrob. Agents. 35*, 322–332.

27 Lambert, P. A. (2002) Mechanisms of antibiotic resistance in Pseudomonas aeruginosa. *J. R. Soc. Med. 95 Suppl 41*, 22–26.

28 Cathcart, G. R. A., Quinn, D., Greer, B., Harriott, P., Lynas, J. F., Gilmore, B. F., Walker, B. (2011) Novel inhibitors of the Pseudomonas aeruginosa virulence factor LasB. A potential therapeutic approach for the attenuation of virulence mechanisms in pseudomonal infection. *Antimicrob. Agents Chemother. 55*, 2670–2678.

29 Zhu, J., Cai, X., Harris, T. L., Gooyit, M., Wood, M., Lardy, M., Janda, K. D. (2015) Disarming Pseudomonas aeruginosa virulence factor LasB by leveraging a Caenorhabditis elegans infection model. *Chem. Biol. 22*, 483–491.

30 Burns, F. R., Paterson, C. A., Gray, R. D., Wells, J. T. (1990) Inhibition of Pseudomonas aeruginosa elastase and Pseudomonas keratitis using a thiol-based peptide. *Antimicrob. Agents Chemother. 34*, 2065–2069.

31 Kessler, E., Israel, M., Landshman, N., Chechick, A., Blumberg, S. (1982) In vitro inhibition of Pseudomonas aeruginosa elastase by metal-chelating peptide derivatives. *Infect. Immun. 38*, 716–723.

32 Kany, A. M., Sikandar, A., Haupenthal, J., Yahiaoui, S., Maurer, C. K., Proschak, E., Koehnke, J., Hartmann, R. W. (2018) Binding Mode Characterization and Early in Vivo Evaluation of Fragment-Like Thiols as Inhibitors of the Virulence Factor LasB from Pseudomonas aeruginosa. *ACS Infect. Dis. 4*, 988–997.

33 Schönauer, E., Kany, A. M., Haupenthal, J., Hüsecken, K., Hoppe, I. J., Voos, K., Yahiaoui, S., Elsässer, B., Ducho, C., Brandstetter, H., Hartmann, R. W. (2017) Discovery of a Potent Inhibitor Class with High Selectivity toward Clostridial Collagenases. *J. Am. Chem. Soc. 139*, 12696–12703.

34 Pereillo, J.-M., Maftouh, M., Andrieu, A., Uzabiaga, M.-F., Fedeli, O., Savi, P., Pascal, M., Herbert, J.-M., Maffrand, J.-P., Picard, C. (2002) Structure and stereochemistry of the active metabolite of clopidogrel. *Drug Metab. Dispos. 30*, 1288–1295.

35 Primi, M. P., Bueno, L., Baumer, P., Berard, H., Lecomte, J. M. (1999) Racecadotril demonstrates intestinal antisecretory activity in vivo. *Aliment. Pharmacol. Ther. 13 Suppl 6*, 3–7.

36 Cushman, D. W., Ondetti, M. A. (1991) History of the design of captopril and related inhibitors of angiotensin converting enzyme. *Hypertension. 17*, 589–592.

37 Pramar, Y., Das Gupta, V., Bethea, C. (1992) Stability of captopril in some aqueous systems. *J. Clin. Pharm. Ther. 17*, 185–189.

38 Adekoya, O. A., Sjøli, S., Wuxiuer, Y., Bilto, I., Marques, S. M., Santos, M. A., Nuti, E., Cercignani, G., Rossello, A., Winberg, J.-O., Sylte, I. (2015) Inhibition of pseudolysin and thermolysin by hydroxamate-based MMP inhibitors. *Eur. J. Med. Chem. 89*, 340–348.

39 Sjøli, S., Nuti, E., Camodeca, C., Bilto, I., Rossello, A., Winberg, J.-O., Sylte, I., Adekoya, O. A. (2016) Synthesis, experimental evaluation and molecular modelling of hydroxamate derivatives as zinc metalloproteinase inhibitors. *Eur. J. Med. Chem. 108*, 141–153.

40 Jacobsen, J. A., Major Jourden, J. L., Miller, M. T., Cohen, S. M. (2010) To bind zinc or not to bind zinc. An examination of innovative approaches to improved metalloproteinase inhibition. *Biochim. Biophys. Acta. 1803*, 72–94.

41 Nishino, N., Powers, J. C. (1980) Pseudomonas aeruginosa elastase. Development of a new substrate, inhibitors, and an affinity ligand. *J. Biol. Chem. 255*, 3482–3486.

42 Browner, M. F., Smith, W. W., Castelhano, A. L. (1995) Matrilysin-inhibitor complexes. Common themes among metalloproteases. *Biochemistry. 34*, 6602–6610.

43 Belviso, B. D., Caliandro, R., Siliqi, D., Calderone, V., Arnesano, F., Natile, G. (2013) Structure of matrix metalloproteinase-3 with a platinum-based inhibitor. *Chem. Commun. (Cambridge, U. K.). 49*, 5492–5494.

44 Holmes, M. A., Matthews, B. W. (1981) Binding of hydroxamic acid inhibitors to crystalline thermolysin suggests a pentacoordinate zinc intermediate in catalysis. *Biochemistry. 20*, 6912–6920.

45 Holland, D. R., Tronrud, D. E., Pley, H. W., Flaherty, K. M., Stark, W., Jansonius, J. N., Mckay, D. B., Matthews, B. W. (1992) Structural comparison suggests that thermolysin and related neutral proteases undergo hinge-bending motion during catalysis. *Biochemistry. 31*, 11310–11316.

46 Overall, C. M., Kleifeld, O. (2006) Towards third generation matrix metalloproteinase inhibitors for cancer therapy. *Br. J. Cancer. 94*, 941–946.

47 Fisher, J. F., Mobashery, S. (2006) Recent advances in MMP inhibitor design. *Cancer Metastasis Rev. 25*, 115–136.

48 Vandenbroucke, R. E., Libert, C. (2014) Is there new hope for therapeutic matrix metalloproteinase inhibition? *Nat. Rev. Drug Discovery. 13*, 904–927.

49 Park, H. I., Jin, Y., Hurst, D. R., Monroe, C. A., Lee, S., Schwartz, M. A., Sang, Q.-X. A. (2003) The intermediate S1' pocket of the endometase/matrilysin-2 active site revealed by enzyme inhibition kinetic studies, protein sequence analyses, and homology modeling. *J. Biol. Chem. 278*, 51646–51653.

50 Rasmussen, H. S., McCann, P. P. (1997) Matrix metalloproteinase inhibition as a novel anticancer strategy. A review with special focus on batimastat and marimastat. *Pharmacol. Ther. 75*, 69–75.

51 Overall, C. M., Kleifeld, O. (2006) Tumour microenvironment - opinion. Validating matrix metalloproteinases as drug targets and anti-targets for cancer therapy. *Nat. Rev. Cancer. 6*, 227–239.

52 Shen, S., Kozikowski, A. P. (2016) Why Hydroxamates May Not Be the Best Histone Deacetylase Inhibitors--What Some May Have Forgotten or Would Rather Forget? *ChemMedChem. 11*, 15–21.

53 Schrump, D. S. (2009) Cytotoxicity mediated by histone deacetylase inhibitors in cancer cells. Mechanisms and potential clinical implications. *Clin. Cancer Res. 15*, 3947–3957.

54 Ruijter, A. J. M. de, van Gennip, A. H., Caron, H. N., Kemp, S., van Kuilenburg, A. B. P. (2003) Histone deacetylases (HDACs). Characterization of the classical HDAC family. *Biochem. J. 370*, 737–749.

55 West, A. C., Johnstone, R. W. (2014) New and emerging HDAC inhibitors for cancer treatment. *J. Clin. Invest. 124*, 30–39.

56 Drummond, D. C., Noble, C. O., Kirpotin, D. B., Guo, Z., Scott, G. K., Benz, C. C. (2005) Clinical development of histone deacetylase inhibitors as anticancer agents. *Annu. Rev. Pharmacol. Toxicol. 45*, 495–528.

57 Chen, C. I.-U., Schaller-Bals, S., Paul, K. P., Wahn, U., Bals, R. (2004) Beta-defensins and LL-37 in bronchoalveolar lavage fluid of patients with cystic fibrosis. *J. Cyst. Fibros. 3*, 45–50.

58 Flemming, H.-C., Wingender, J. (2010) The biofilm matrix. *Nat. Rev. Microbiol. 8*, 623–633.

59 Whitchurch, C. B., Tolker-Nielsen, T., Ragas, P. C., Mattick, J. S. (2002) Extracellular DNA required for bacterial biofilm formation. *Science. 295*, 1487.

60 Lewenza, S. (2013) Extracellular DNA-induced antimicrobial peptide resistance mechanisms in Pseudomonas aeruginosa. *Front. Microbiol. 4*, 21.

61 Haupenthal, J., Baehr, C., Zeuzem, S., Piiper, A. (2007) RNAse A-like enzymes in serum inhibit the anti-neoplastic activity of siRNA targeting polo-like kinase 1. *Int. J. Cancer. 121*, 206–210.

62 Winter, G. (2010) xia2. An expert system for macromolecular crystallography data reduction. *J. Appl. Crystallogr. 43*, 186–190.

63 McCoy, A. J., Grosse-Kunstleve, R. W., Adams, P. D., Winn, M. D., Storoni, L. C., Read, R. J. (2007) Phaser crystallographic software. *J. Appl. Crystallogr. 40*, 658–674.

64 Emsley, P., Lohkamp, B., Scott, W. G., Cowtan, K. (2010) Features and development of Coot. *Acta Crystallogr., Sect. D: Biol. Crystallogr. 66*, 486–501.

65 Adams, P. D., Afonine, P. V., Bunkóczi, G., Chen, V. B., Davis, I. W., Echols, N., Headd, J. J., Hung, L.-W., Kapral, G. J., Grosse-Kunstleve, R. W., McCoy, A. J., Moriarty, N. W., Oeffner, R., Read, R. J., Richardson, D. C., Richardson, J. S., Terwilliger, T. C., Zwart, P. H. (2010) PHENIX. A comprehensive Python-based system for macromolecular structure solution. *Acta Crystallogr., Sect. D: Biol. Crystallogr. 66*, 213–221.

66 Skubák, P., Murshudov, G. N., Pannu, N. S. (2004) Direct incorporation of experimental phase information in model refinement. *Acta Crystallogr., Sect. D: Biol. Crystallogr. 60*, 2196–2201.

67 Krieger, E., Koraimann, G., Vriend, G. (2002) Increasing the precision of comparative models with YASARA NOVA--a self-parameterizing force field. *Proteins. 47*, 393–402.

68 Thomann, A., Mello Martins, A. G. G. de, Brengel, C., Empting, M., Hartmann, R. W. (2016) Application of Dual Inhibition Concept within Looped Autoregulatory Systems toward Antivirulence Agents against Pseudomonas aeruginosa Infections. *ACS Chem. Biol. 11*, 1279–1286.

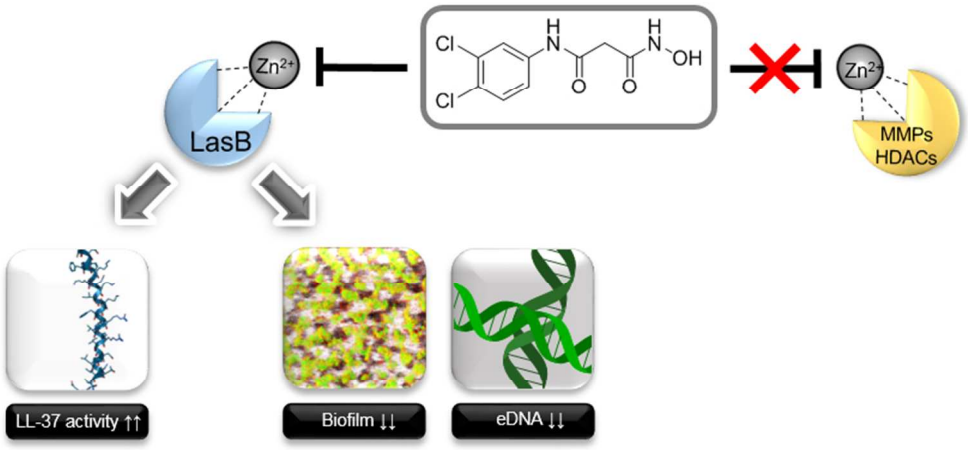

141x68mm (150 x 150 DPI)